pH Dependence of the Properties of Waterborne Pressure-Sensitive Adhesives Containing Acrylic Acid

Tao Wang, Elisabetta Canetta, Tecla G. Weerakkody, and Joseph L. Keddie*

Department of Physics and Surrey Materials Institute, University of Surrey, Guildford, Surrey GU2 7XH, United Kingdom

Urko Rivas

Institute for Polymer Materials (POLYMAT) and Grupo de Ingeniería Química, Departamento de Química Aplicada, University of the Basque Country, Joxe Mari Korta Zentroa, Tolosa Etorbidea 72, 20018 Donostia-San Sebastián, Spain

ABSTRACT Polymer colloids are often copolymerized with acrylic acid monomers in order to impart colloidal stability. Here, the effects of the pH on the nanoscale and macroscopic adhesive properties of waterborne poly(butyl acrylate-*co*-acrylic acid) films are reported. In films cast from acidic colloidal dispersions, hydrogen bonding between carboxylic acid groups dominates the particle–particle interactions, whereas ionic dipolar interactions are dominant in films cast from basic dispersions. Force spectroscopy using an atomic force microscope and macroscale mechanical measurements show that latex films with hydrogen-bonding interactions have lower elastic moduli and are more deformable. They yield higher adhesion energies. On the other hand, in basic latex, ionic dipolar interactions increase the moduli of the dried films. These materials are stiffer and less deformable and, consequently, exhibit lower adhesion energies. The rate of water loss from acidic latex is slower, perhaps because of hydrogen bonding with the water. Therefore, although acid latex offers greater adhesion, there is a limitation in the film formation.

KEYWORDS: latex • film formation • adhesion • adhesives • acrylic acid • pH

1. INTRODUCTION

Latex is an aqueous colloidal dispersion of polymer particles used as building blocks for coatings and adhesives (1, 2). Being waterborne, the materials offer a means of processing that does not emit volatile organic compounds into the atmosphere. Polymer colloids offer a distinct advantage over other classes of materials because they enable the structure to be tailored and controlled at the nanoscale. Particles can contain two or more phases and have a prescribed structure, such as core–shell (3). Upon drying of monosized latex particles, a dodecahedral (honeycomb) structure (4, 5) is created in the film formation process (6, 7).

The boundaries between the particles have an enormous area. The properties of the boundary region therefore can have a profound influence on the macroscale properties of latex films. For instance, the boundary region has been tuned by the introduction of cross-linking between adjacent shells in a core–shell latex film (8). The covalent bonds at the boundaries between latex particles, which formed a continuous network throughout the film, had a pronounced influence on the mechanical and adhesive properties of the resulting films. This present work considers weaker bonding at interfaces, rather than the covalent bonding in the core–shell latex films.

In most latex applications, several monomers are incorporated into the polymer by copolymerization, in order to impart the desired properties. Acrylic acid (AA) or methacrylic acid is often used in both coating (9) and adhesive (10, 11) formulations. These monomers' carboxylic acid groups provide colloidal stability in the wet latex through electrosteric stabilization at higher pH values when they are negatively charged. Carboxylic acid (COOH) groups impart hydrophilicity; therefore, acidic monomers tend to concentrate at the particle surface during emulsion polymerization, with the more hydrophobic monomers being localized within the particle cores. Upon film formation, the hydrophilic layer around the particle evolves into a continuous phase in which the hydrophobic cores are encapsulated (12).

Polymers or copolymers that contain carboxylic acid groups are known to be pH-responsive. The apparent pK_a value (defined as the pH with 50% ionization) of poly(acrylic acid) (PAA), which is of interest here, is ca. 5.8 (13). When $pH < pK_a$, the carboxylic acid in PAA is not dissociated, and it is known to be capable of participating in hydrogen bonding as a donor and in the absence of water (14–16). When $pH > pK_a$, the groups are deprotonated to create negatively charged COO^- groups. As the pH increases from acidic to basic, the carboxylic acid groups dissociate, leading

* Corresponding author. Tel: +44 1483 686803. Fax: +44 1483 686781. E-mail: j.keddie@surrey.ac.uk.
Received for review November 15, 2008 and accepted February 16, 2009
DOI: 10.1021/am800179y

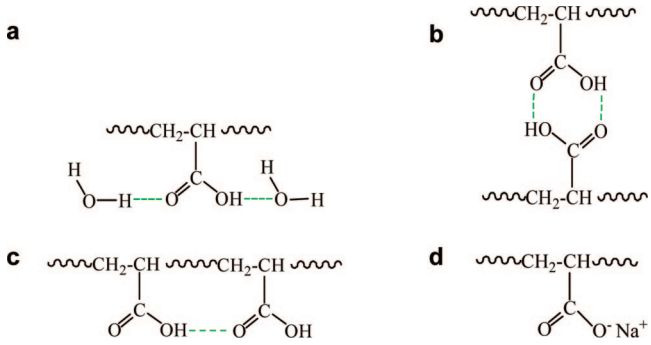

FIGURE 1. Molecular interactions of P(BuA-*co*-AA) drying and dried latex films: (a) hydrogen bonds between COOH groups and water molecules (15); (b) dimers between COOH groups (16); (c) lateral hydrogen bonds between COOH groups; (d) ionic dipole created by COO^- and Na^+ counterions.

to the loss of its hydrogen-bonding capability, accompanied by an increasing amount of ionization.

The various types of possible interactions involving COOH are illustrated in Figure 1 (15−17). At lower pH values, there is hydrogen bonding between the COOH-rich particle surface and water (15) (Figure 1a). There can also be hydrogen bonding between two particle surfaces in close contact, leading to the creation of dimers (Figure 1b). At higher pH values, counterions will balance the charge of COO^- groups, creating neutral dipoles, such as is illustrated in Figure 1d.

Extensive previous research (18−22) has been carried out on high glass transition temperature (T_g) latex films (i.e., T_g comparable to, or greater than, room temperature) containing AA comonomers for coatings applications. The presence of the hydrophilic AA groups imparts colloidal stability in the wet state, and interactions between the groups have pronounced effects on various physical properties, e.g., viscoelasticities (18−20), polymer diffusion (21), and barrier properties (21, 22) in the dry films.

Carboxylated styrene−butadiene (SB) copolymer latex films have been the subject of dynamic mechanical analysis (DMA) as a function of the pH (18, 20). Richard and Maquet (18) proposed that, in acidic latex films, dimers created by hydrogen bonding between COOH groups acted as cross-links at the particle interfaces. They found that the elastic moduli of latex films increased with the COOH concentration on the latex particle surfaces. At basic pH values, the latex resulted in films with higher elastic moduli. The authors proposed that the counterions that neutralized the carboxylate groups at high pH values resulted in dipoles. They attributed the higher moduli to "ionic dipolar interactions". They proposed that monovalent (not only di- or trivalent) ions can participate in these dipolar interactions, which lead to a type of interfacial cross-linking. Kan and Blackson (20), on the other hand, explained the higher elastic modulus at high pH values in terms of a higher T_g in the interfacial region and the accompanying reduced molecular mobility, when the ionomers were neutralized with counterions.

In pressure-sensitive adhesive applications, for which the polymer must have a low T_g, copolymers containing AA are often used. The influence of the presence of AA on the adhesive properties of latex films has been proven beyond doubt (10). In a preliminary study on adhesives (23), it was also shown that the pH value of a poly(butyl acrylate) latex containing methacrylic acid groups has an effect on the macroscopic tack adhesion of the resulting latex films. However, no extensive and systematic studies of how the pH of a low-T_g latex affects the interparticle interactions, and, in turn, the film drying, mechanical properties, and adhesion, have been reported. A systematic study is required in order to formulate a design principle for emulsion copolymerization for various applications.

Here, a poly(butyl acrylate-*co*-acrylic acid) [P(BuA-*co*-AA)] latex, which is suitable as a model pressure-sensitive adhesive, is studied. The particle surfaces are enriched with PAA. We explore how the pH of the wet latex influences the molecular interactions in the dry films and how, in turn, these determine the mechanical and tack properties at both the nano- and macroscale.

2. EXPERIMENTAL DETAILS

2.1. Materials. The P(BuA-*co*-AA) latex was prepared by emulsion polymerization of *n*-butyl acrylate and AA (99:1, w/w), as described elsewhere (24). Sodium dodecyl sulfate (SDS; 2 wt % on the monomer) was used as the emulsifier and potassium persulfate (0.25 wt %) as the initiator. The average particle size was 120 nm, and the T_g of the copolymer was ca. −50 °C. The final solids content was 50 wt %, and the gel content was 30%, according to Soxhlet extraction in tetrahydrofuran. The pH of the standard P(BuA-*co*-AA) latex dispersions was 6.8. The free surfactant concentration in the latex serum was estimated to be 0.35 g L^{-1} through Du Nouy ring tensiometry (KSV Sigma 70 surface tensiometer, KSV Instruments Ltd.) of the serum that had been separated from the latex through ultracentrifugation.

The fraction of carboxylic acid groups at the surface of the particle was determined by conductometric titration. Because the latex was neutralized with ammonia just after it was synthesized, it was necessary to remove the ammonia by devolatilization prior to the titration. In this procedure, the pH of the latex was adjusted to 10 with NaOH to shift the ammonium−ammonia equilibrium toward the ammonia. Once the sample was free of ammonia, HCl was added until a pH lower than 2 was reached. Then the sample was titrated with NaOH, which reacted first with the strong acids and then with the carboxylic acid groups. It was found that the amount of AA at the particle surface was 20% of the total AA in the formulation. To investigate the pH effects on the mechanical properties, the pH was subsequently adjusted by the dropwise addition of 1 M HCl, 1 M NaOH, or 1 M NH_4OH solutions in water.

2.2. Fourier Transform Infrared (FTIR) Spectroscopy. FTIR spectra of dried free-standing latex thin films were obtained by using an FTIR spectrometer (Perkin-Elmer system 2000 FTIR; Waltham, MA) from 500 to 4000 cm^{-1} at a resolution of 4 cm^{-1} from an average of 64 scans.

2.3. AFM Force Spectroscopy. Latex films (ca. 50 μm thick) consisting of >400 particle layers were deposited onto freshly cleaved mica sheets by spin coating at 500 rpm. The nanomechanics of the surfaces were investigated by performing force spectroscopy in contact mode using a commercial atomic force microscope (AFM) (NTEGRA, NT-MDT, Moscow, Russia) with Si_3N_4 cantilevers (CSG10, NT-MDT, Moscow, Russia) having a nominal spring constant of 7 N m^{-1} and a nominal resonant frequency of 35 kHz. The AFM conical tip (radius of curvature of 10 nm) indented the latex film by an indentation depth, δ, of less than 1 μm, leading to a small contact area between the tip and the sample (indentation cycle). The sample was then lowered away from the tip (sample scan configuration) at a

constant speed of 0.45 μm s^{-1}, while a force spectroscopy curve was recorded (retraction cycle) (25). In total, 25 curves (consisting of a trace and retrace) were recorded in a grid covering an area of 2 μm × 2 μm. During the whole experiment, an average normal force of 4 nN was applied by the AFM cantilever. All experiments were performed at a room temperature of ca. 25 °C.

Force F versus the sample displacement data were transformed into force−distance (F−d) curves through shifting of the sample displacement by the indentation depth, δ. During the retraction cycle, the deflection of the cantilever, z, was up to a few tens of nanometers and, therefore, was negligible in comparison to the deformation undergone by the polymer over several micrometers. Because of the small contact area between the AFM tip and the sample, the adhesive force contribution during the indentation cycle is considered to be negligible. The maximum separation force of the tip from the sample surface (F_s), the maximum distance of deformation (d_{max}), and the separation energy (E_s), defined as the area under a curve, were measured from the F−d retrace curves. An elastic modulus of the latex film surface, E, was extracted through inversion of a reasonable analytical approximation (26) given as

$$F = \frac{2\tan(\alpha)E\delta^2}{\pi(1-\upsilon^2)} \quad (1)$$

where F is the force exerted by the AFM tip onto the polymer surface during the *indentation* cycle, α is the half-opening angle of the tip (taken here as 11°), and υ is Poisson's ratio of the sample, which is assumed to be 0.5 for an incompressible polymer. The maximum indentation, δ_{max}, and the corresponding force, F_{max}, were used in the calculation. Equation 1 neglects any consideration of the effect of any attractive adhesive forces between the AFM tip and the surface, which will increase the contact area between the two beyond what is the result of elastic deformation alone (27). If the true contact area is greater than what is assumed, the calculated E will be greater than what is found from those analytical expressions that consider adhesive contributions (27, 28). The value of E obtained using eq 1 will be hereafter referred to as an effective modulus, E_{eff}, to reflect the fact that consideration of the effect of any adhesive forces has been neglected.

2.4. Macroscale Probe−Tack Analysis. Films were cast onto glass plates at room temperature using a cube applicator and allowed to dry at 50 °C in an oven under flowing air for half an hour prior to analysis. The dry film thickness, h, was around 60 μm and was measured before each experiment. Probe−tack experiments were performed following the Avery method on a commercial apparatus (MicroSystems Texture Analyzer, Godalming, U.K.) using a spherical polypropylene (PP) probe (1). This probe material was chosen because of its low surface free energy (ca. 0.02 J m^{-2}) (29), which presents a greater challenge in obtaining high adhesion energy values. The probe was pressed into contact with the film under a load of 4.9 N for 1 s before being retracted at a constant velocity of 100 μm s^{-1}, corresponding to an initial strain rate of 1.7 Hz. The radius of the PP probe, R, was 12.5 mm. The radius of the maximum circular contact area between the probe and the polymer films, a, was typically 0.9 mm. For each experiment, a was measured and used in the calculation of the engineering stress (defined as the force divided by πa^2). The strain is defined as the change in the film thickness divided by its initial value: $\Delta h/h$.

2.5. Macroscale Mechanical Analysis. The latex dispersions were deposited in Teflon molds and allowed to dry for 7 days before removing them to obtain a thick (ca. 1 mm) free-standing film. Tensile specimens (10 mm × 1 mm × 1 mm) were cut from the dry films. Tensile stress−strain measurements were carried out with a commercial instrument (Stable Micro Systems Ltd., Godalming, U.K.) with a constant strain velocity of 5 mm s^{-1}, corresponding to an initial strain rate of ca. 0.5 Hz. Three replicate experiments were performed. To determine the energy dissipation rate and modulus, similar specimens were used for DMA (Q800, TA Instruments, New Castle, DE) in tensile mode with a strain of 0.25% and a frequency of 1 Hz over a temperature range from −80 to +50 °C. The frequency is comparable to the strain rate in the tensile and tack measurements.

2.6. Gravimetric Analysis of Drying. Wet films were cast onto clean glass coverslips (18 mm × 18 mm) with a wet thickness of around 200 μm. Gravimetric analysis of water loss during latex drying was performed by placing the sample on a digital balance. The weight of the sample was recorded every 2 min over a period of 3 h. The room humidity was 40%, and the air above the sample was static.

3. RESULTS AND DISCUSSION

3.1. Molecular Interactions of Latex Films. IR spectra of PAA in water, obtained by Kaczmarek and coworkers (15), showed that lateral hydrogen bonds between COOH groups (as in Figure 1c) have a characteristic stretching band ranging between 1669 and 1679 cm^{-1}, depending on the concentration and the buffer. The stretching band of the COOH dimer is reported to be at 1712 cm^{-1}, and the stretching band of free C═O is at 1739 cm^{-1}. A band centered at 1542 cm^{-1} is assigned to the antisymmetric ν_a(COO$^-$) stretching vibration of carboxylate groups (15).

Figure 2 illustrates the FTIR spectra obtained from dry P(BuA-*co*-AA) films cast from dispersions with different pH values. The films are of an identical thickness. These spectra have several shifts in the wavenumber due to various intermolecular interactions between the chemical components. In Figure 2a, the latex film cast at a pH of 4 shows a peak centered around 1672 cm^{-1}, which is attributed to lateral hydrogen bonds of COOH groups. This peak is stronger in comparison to the peak obtained from the latex film at pH 9.0, indicating the formation of more lateral hydrogen bonds in the former.

In Figure 2b, a band centered around 1729 cm^{-1} is observed in all spectra. This band is assigned to the free C═O stretching. It is weaker in the film cast at a pH of 4.0, which indicates that the concentration of free C═O groups is lower in this film because parts of the groups participate in hydrogen bonding. Drawing on the literature (15), one would expect the appearance of a band for the COOH dimers in the region around 1712 cm^{-1}, but it is not observed here. However, the asymmetry observed in the 1729 cm^{-1} band could be caused by convolution with the COOH dimer band. In any case, there is no observable difference with changing pH.

Increasing the pH above the pK_a value is expected to lead to ionization of the carboxylic acid group. We attribute the band at 1542 cm^{-1} in Figure 2c to the presence of negatively charged COO$^-$ groups. The strength of this band increases as the pH increases from 4 to 9, which is consistent with the presence of more of these groups, with their charge balanced by Na$^+$ counterions.

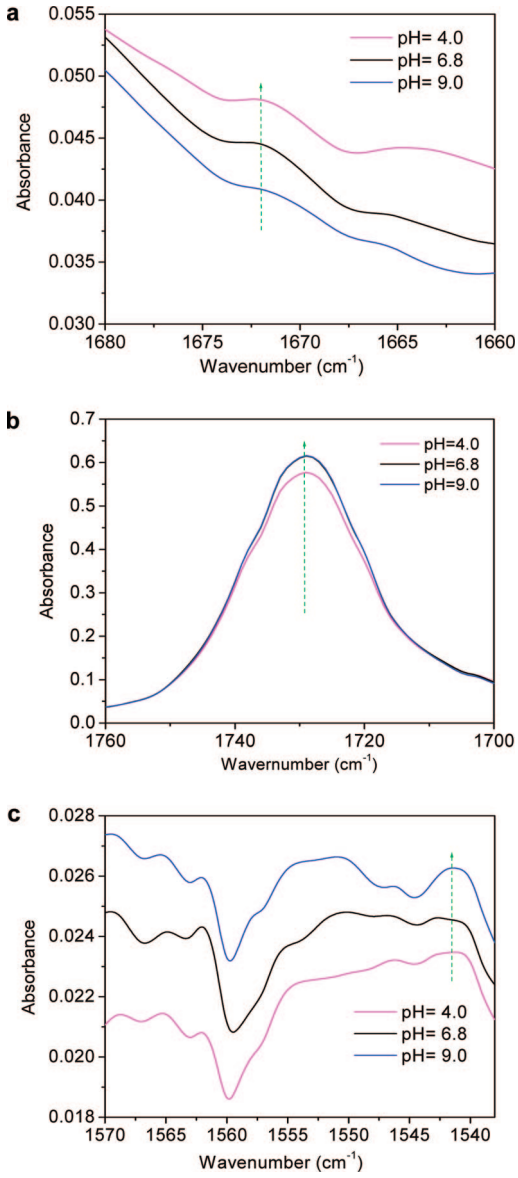

FIGURE 2. FTIR absorbance spectra of dried latex films cast from dispersions with three different pH values, as indicated in the legend for three different spectral regions: (a) lateral COOH bond characteristic region; (b) free C═O stretching and COOH dimer regions; (c) ionic interaction characteristic region. The spectra in parts a and c were shifted vertically for clarity.

These results reveal that the pH of the latex dispersion has an influence on the final bonding interactions in the dry films, which is consistent with the findings of previous research (18−20). At a pH of 4, the data indicate that hydrogen bonding is dominant. At a pH of 9, adjusted by NaOH, there is some evidence for the formation of dipoles, in which the negative charge of the COO^- groups is balanced by the Na^+ cations. Hereafter, the influence of the observed hydrogen bonding and ionic dipolar interactions on the low T_g film properties is reported.

3.2. AFM Force Spectroscopy of Latex Films. AFM force spectroscopy allows the study of adhesion and deformation of single latex particles, particle monolayers, or multilayers (30−33). In our experiments, good reproducibility of the force spectroscopy traces was found, which indicates that surfactants either at the film surface or in the bulk do not cumulatively affect the nanoadhesive properties. There is no evidence for contamination of the tips by the surfactant during a series of force spectroscopy measurements. Figure 3 shows representative $F-d$ curves obtained from latex films cast at three pH values, and hence with varying levels of hydrogen bonding or ionic interactions between particles.

The $F-d$ retrace curves (Figure 3) show a rigid response at small tip−polymer distances until reaching a maximum separation force, F_s. Then the polymer yields with a continuously decreasing force until the release of the tip from the surface. Because of the large film thickness ($\gg 1$ μm) used in this work, the retrace curve demonstrates a monotonic shape rather than a steplike shape, as has been previously reported in the literature for polymer films (several hundreds of nanometers thick) (30, 31). Previous studies of latex deformation with nanoscale thickness also showed a displacement of several hundreds of nanometers before the AFM tip detached from latex particle surfaces (30, 31).

Table 1 summarizes the nanomechanical properties of the latex films determined by analysis of the $F-d$ curves, such as is presented in Figure 3. The mean values of 25 measurements (±standard deviation) are reported. The latex film with hydrogen-bonding interaction (pH of 4) shows an E_{eff} of 1.8 MPa, whereas the latex film with ionic dipolar interactions (pH of 9, adjusted by NaOH) exhibits a significantly higher E_{eff} of 3.0 MPa. With hydrogen-bonding interactions between particles, the retrace curve shows an F_s of around 300 nN and a d_{max} of 5.5 μm (Figure 3a). The $F-d$ curve of the latex film with ionic dipolar interactions (Figure 3c), on the other hand, shows a higher F_s of 380 nN but a shorter d_{max} of only 2.5 μm. (Note that the retrace curve starts at a negative value.) These results indicate that the contribution of the hydrogen-bonding interactions to the film stiffness and cohesion at the surface is less than the contribution from ionic dipolar interactions. In addition, greater extensibility is obtained with hydrogen-bonding interactions.

An additional experiment was performed to determine the role of the counterion in determining the mechanical properties of the latex films. The pH was adjusted to 9 using NH_4OH. In aqueous solution, there will be an equilibrium between $NH_4^+ + OH^-$ and aqueous $NH_3 + H_2O$. During the drying process, NH_3 will evaporate and therefore reduce the concentration of NH_4^+ counterions in solution. The effect of NH_3 evaporation leading to a pH drop and protonation of carboxylate groups has been proposed by Feng and Winnik (21). Experimental measurements of the pH in latex that contains NH_4OH have found a decrease that is attributed to NH_3 evaporation (34).

The F_s value of latex films pH-adjusted with NH_4OH is only 310 nN and is close to the 300 nN of latex films cast from a latex with a pH of 6.8. The ionic dipolar interactions are presumed to be diminished, and consequently there is depressed film cohesion. With NH_4OH pH adjustment, d_{max} is likewise comparable to what is found at a pH of 6.8, showing greater extensibility compared to the NaOH case.

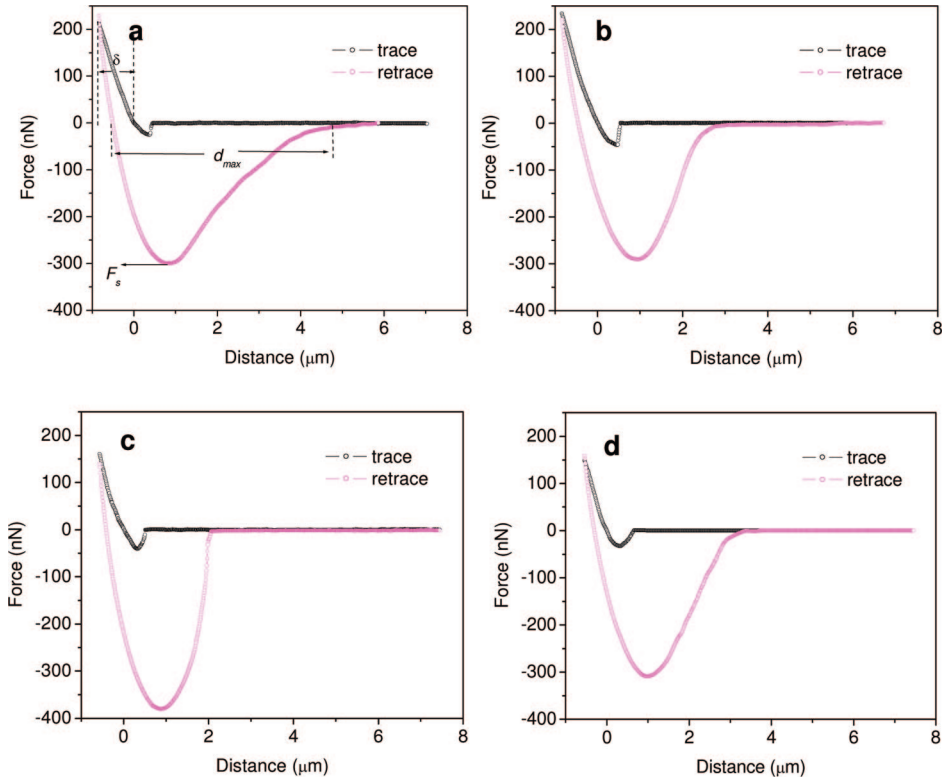

FIGURE 3. AFM $F-d$ curves from latex films cast from different pH dispersions: (a) pH 4.0; (b) pH 6.8; (c) pH 9.0 adjusted with NaOH; (d) pH 9.0 adjusted with NH_4OH.

Table 1. AFM Force Spectroscopy Data of Latex Films Cast from Different pH Values

pH	maximum separation force, F_s (nN)	maximum distance, d_{max} (μm)	effective elastic modulus, E_{eff} (MPa)	separation energy, E_s ($\times 10^{-13}$ J)
4.0	300 ± 20	5.5 ± 1.0	1.8 ± 0.4	7.8 ± 1.0
6.8	300 ± 15	3.2 ± 0.3	2.0 ± 0.2	5.8 ± 0.3
9.0 (by NaOH)	380 ± 18	2.5 ± 0.2	3.0 ± 0.2	6.7 ± 0.3
9.0 (by NH_4OH)	310 ± 20	3.2 ± 0.2	2.6 ± 0.2	6.2 ± 0.3

E_s is a function of the adhesion energy between the tip and the surface coupled with the energy required to deform the polymer. Table 1 shows that the film cast at a pH of 4 (dominated by hydrogen-bonding interactions) has the highest E_s of around 7.8×10^{-13} J. This greater separation energy is associated with a greater deformability (high d_{max}). The stiffer (high-modulus) latex films obtained at higher pH values are less deformable and show a lower E_s.

E_s values presented in Table 1 correspond to different contact areas between the AFM tip and the film, with stiffer films leading to smaller contact areas than softer ones because of a less deep indentation in the former. Indeed, the different indentation depths presented in Figure 3 support this point. For example, the indentation depths in parts a and b of Figure 3 are 0.84 and 0.56 μm, respectively. A larger contact area was achieved with a deeper indentation. Although the separation energies are related to the adhesion energies, they are not expected to be identical.

An important conclusion is that force spectroscopy is strongly dependent on the particle−particle interactions and not just the tip−surface interactions. The results indicate that hydrogen-bonding and ionic dipole interactions between the particles contribute to the force spectroscopy data.

3.3. Macroscale Adhesive Properties. The macroscale adhesive properties of the latex films with different particle interactions were determined from probe−tack measurements. Three representative probe−tack curves are presented in Figure 4a for films cast from latex dispersions with pH values of 4.0, 6.8, and 9.0. Previous studies on pressure-sensitive adhesives have provided detailed interpretations of the meaning of stress−strain relationships in the probe−tack curves (1, 35−38). Cavities will form either at the probe−film interface or in the bulk of the adhesive film, as a result of negative pressure in the film (39, 40). The number of cavities reaches a maximum around the peak of the stress−strain curve. As the cavities propagate laterally or vertically, the stress falls to a plateau level. As the cavities expand, the walls between them are drawn into fibrils. The stress level in the plateau region is determined by the force to draw the fibrils. The detachment of the fibrils leads to the stress dropping to zero. If the fibrils fail cohesively, the stress usually falls more gradually, as the fibrils grow thinner and break.

The stress−strain curve of the latex with hydrogen-bonding interactions (pH of 4) shows a much longer plateau compared with the adhesive made from a latex dispersion with ionic interactions (pH of 9). Consequently, the greatest adhesion energy is obtained. The length of the plateau indicates that the polymer has an appropriate viscoelasticity to allow the drawing of fibrils. It is not too stiff, and the stress level indicates that the polymer is not too liquidlike. The

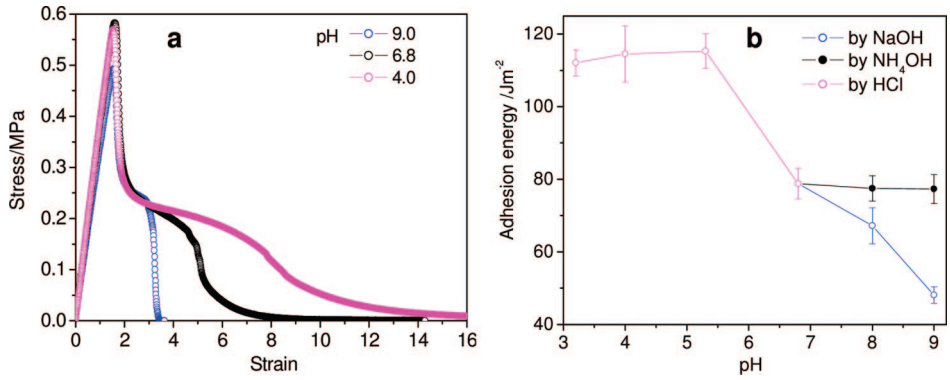

FIGURE 4. (a) Probe−tack curves showing engineering stress as a function of the strain and (b) adhesion energy of the latex films as a function of the pH values of the dispersion. The legend in part a indicates the pH value of the latex used to cast the adhesive. The legend in part b indicates how the pH was adjusted.

adhesive made from latex dispersion at a pH of 9.0, adjusted by NaOH, shows a very narrow shoulder rather than a plateau and a lower adhesion energy. Fibrils are not drawn very far.

The adhesion energy as a function of the pH of the latex dispersions is summarized in Figure 4b. With hydrogen-bonding interactions (in the low pH range), the adhesion energy is around 110 J m^{-2}. When the latex pH is above the pK_a of PAA, the adhesion energy begins to drop, as ionic interactions start to contribute to the particle−particle interactions. With a further increase in the pH, the PAA groups at the latex particle surfaces are further ionized. This leads to a continuous decrease of the adhesion energy. At a pH of 9.0, adjusted by NaOH, the adhesion energy is around 50 J m^{-2}. As a comparison, the adhesion energy of the adhesive films cast from a latex dispersion at a pH of 9.0, adjusted by NH_4OH, remains around 78 J m^{-2}. An explanation is that NH_4OH decomposed to NH_3 and evaporated during the film drying process. Therefore, a counterion effect is not active in the film.

The trend in these macroscale measurements of adhesion tack energy is consistent with the one observed in the AFM separation energy. Elsewhere, AFM nanomechanical analysis on a soft latex also demonstrated that relatively weak interparticle junctions can improve tackiness (41).

A full explanation of these adhesion results requires further information about the macroscale mechanical deformation and the viscoelasticity of the latex films. Tensile deformation and DMA were performed on films with different particle interactions adjusted by the pH.

The tensile deformation properties of the latex film, which were determined from thick film strips, are compared in Figure 5a. The latex film cast at a pH of 4 demonstrates the lowest elastic modulus (measured from the curve's slope at small strains) and the greatest strain at failure. The latex film cast at a pH of 9 adjusted by NaOH (with dominant ionic interactions), however, has a much higher modulus with a smaller strain at failure. Previous work (18−20) on the macroscale deformation properties of high T_g latex films with different particle interactions also showed that ionic interactions lead to a more rigid response, compared to that of hydrogen-bonding interactions. The stress−strain curve of a pH 9 film adjusted by NaOH demonstrates some strain-hardening, while the pH 4 film demonstrates a strain-softening character after the yield point. Recall that the $F-d$ curves from AFM showed similar mechanical behavior. During the failure, the force degrades gradually over a long distance in the pH 4 latex, whereas the force falls abruptly at the maximum separation force in the pH 9 latex adjusted by NaOH. Hence, the macroscale tensile deformation is consistent with the nanoscale deformation properties.

As further evidence for the counterion effect, when NH_4OH was used to raise the pH, there is a negligible mechanical strengthening effect. The modulus, strength, and maximum strain stay around the values for the pH 6.8 film. When NH_3 evaporates, there are fewer cations and the ionic dipolar interactions are less significant. Similarly, Kan and Blackson (20) reported a lower elastic modulus in the SB latex that was neutralized with NH_4OH rather than NaOH.

The DMA of the various latex films is shown in Figure 5b,c. Table 2 summarizes the key dynamic mechanical parameters. The latex film with hydrogen-bonding interactions (pH of 4) has a low modulus (0.28 MPa) but a high tan δ. The breaking of hydrogen bonds within the acidic latex films might provide an additional energy dissipation mechanism, which leads to higher tan δ. The pH 9 (NaOH) latex films, on the other hand, show the highest modulus (0.52 MPa) but an intermediate tan δ value. In this case, ionic interactions are stiffening the latex significantly.

The modulus has a pronounced effect on the adhesive properties. As stated in the Dahlquist criterion (42) and experimentally demonstrated (24), a pressure-sensitive adhesive must have a modulus that is not too high. Otherwise, it will not sufficiently wet the adherend. A modulus of 0.52 MPa, as reported above, is higher than the acceptable range.

The ratio of tan δ over the storage modulus (E') of an adhesive can be used as a gauge of the adhesion energy. In general, the tan δ/E' value is proportional to the adhesion energy of pressure-sensitive adhesives (24, 43, 44). The experimental ratio can be used to explain the adhesive results. The tan δ/E' ratio at room temperature for the pH 4 latex has the highest value (0.85), and it likewise has the highest adhesion energy (110 J m^{-2}). The tan δ/E' value is higher when the pH is adjusted by NH_4OH in comparison to

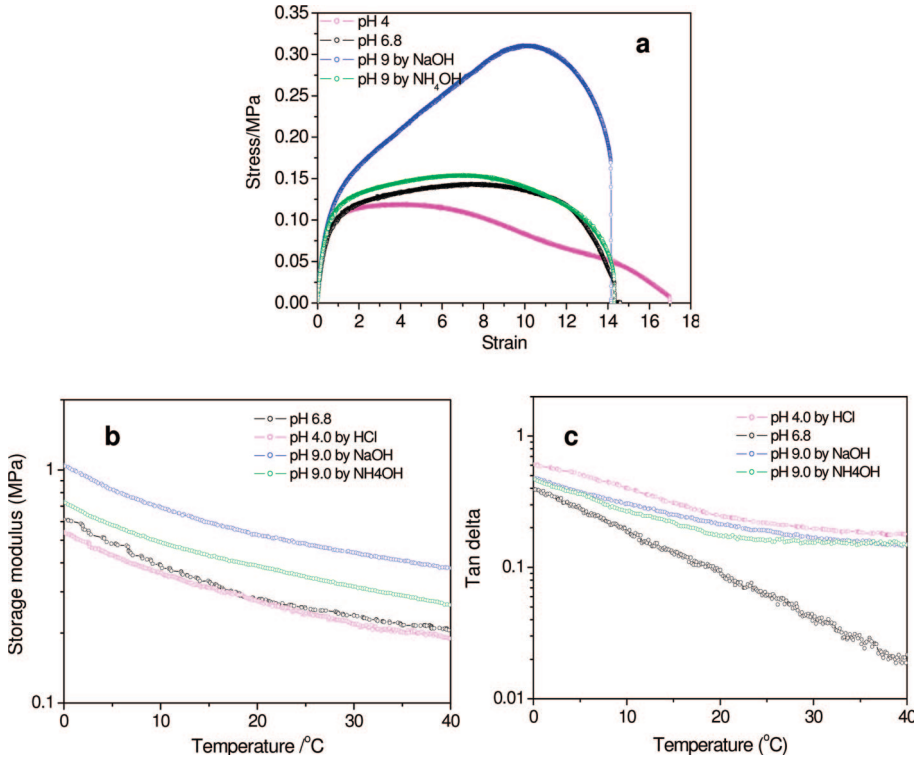

FIGURE 5. (a) Macroscale tensile deformation of latex films cast at three different pH values as indicated in the legend. Temperature dependence of the (b) storage moduli, E', and (c) tan δ obtained by DMA on the same materials.

Table 2. Correlation of the Moduli of Latex Films from DMA and Macroscopic Adhesion Energies[a]

latex pH	storage modulus, E' (MPa)	tan δ	tan δ/E' (MPa^{-1})	probe–tack adhesion energy (J m^{-2})
4.0	0.28	0.24	0.85	115
6.8	0.28	0.10	0.36	79
9.0 by NaOH	0.52	0.21	0.40	48
9.0 by NH_4OH	0.39	0.18	0.45	77

[a] tan δ and E' were obtained at 20 °C.

NaOH, which is consistent with the observed trend in the adhesion energy.

As an empirical conclusion, a soft material with a tan δ/E' value in the range from 0.4 to 1 MPa^{-1} will demonstrate a high adhesion energy and will function as a high-performance adhesive, providing that the elastic modulus meets the Dahlquist criterion. A high tan δ/E' of 1 MPa^{-1} is, however, difficult to achieve for viscoelastic polymers employed as pressure-sensitive adhesives. Viscous liquids, e.g., oil or honey, with liquidlike rheological behavior (loss modulus higher than the storage modulus) certainly have a very high tan δ/E' value, but their moduli are too low to provide enough cohesion to be effective pressure-sensitive adhesives.

We note that the moduli of the adhesive films can also be extracted from the probe–tack measurements using the large spherical indenter. The modulus can be extracted from a complex relation of the modulus with the loading force, radius of the probe, and radius of the maximum contact area. The method has been reviewed by Shull (27). The readers are referred to this reference for details.

The absolute values of the moduli from force spectroscopy and macroscale DMA are different, but they demonstrate the same trend caused by different interactions. It is fair to say that force spectroscopy on micrometer-thick latex films can reveal trends in macroscopic mechanical properties. It has been demonstrated elsewhere that the moduli determined by this method compared favorably with macroscopic results (45). The differences between the absolute values obtained in this work by force spectroscopy and by macroscale measurements are caused by several factors. The effective elastic modulus, E_{eff}, has ignored the effect of the adhesive forces between the AFM tip and the film by using eq 1. Another significant factor is that eq 1 applies to the indentation experiments performed with a conical tip. If the shape of the tip is less sharp, for example, a parabolic or hyperbolic shape, different formulas should be applied to calculate the elastic modulus (26). There might be a minor effect caused by the different frequencies of the two techniques. The AFM nanoindentation has an initial frequency of around 0.5 Hz, while the macroscale DMA has a constant frequency of 1 Hz.

3.4. Rate of Water Loss. Both AFM nanomechanics and macroscale probe–tack measurements show that a low pH with hydrogen bonding gives the highest debonding energy (as indicated by the separation energy and the tack adhesion energy, respectively). It is necessary to evaluate the film formation process of the latex at various pH values to determine the feasibility of using the low pH latex in an application.

Figure 6 shows the water fraction as a function of the normalized drying time for dispersions of P(BuA-*co*-AA) from

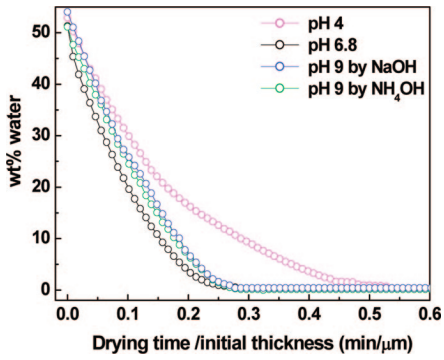

FIGURE 6. Gravimetric analysis of water loss from latex films at different pH values, as indicated.

pH 4, 6.8, and 9 by NaOH and pH 9 by NH_4OH. To take into account small variations in the film thicknesses, the drying time has been normalized by the initial film thickness. Up until a normalized time of 0.1, each of the four latex films loses water at the same rate. During this early stage of drying, there is free evaporation of water. At longer times, when there is less than 20 wt % water and the polymer particles are in close contact, the rate of water loss slows in the latex at a pH of 4. A possible explanation is the predominance of hydrogen-bonding interactions (as is illustrated in Figure 1a) that bind with water at the particle boundaries. These restricted water molecules evaporate much more slowly, and the latex film therefore takes a longer time to reach the dry stage.

These results on drying can also be considered in light of previous research on water uptake by high-T_g latex films that contain carboxylic groups. Dry latex films that contain methacrylic acid (21) or AA (19) have been shown to absorb a larger amount of water (from vapor or liquid) when neutralized with NaOH rather than when in the acid state containing COOH. These results were attributed to the greater hydrophilicity imparted by ionic dipoles of COO^- and Na^+. These observations suggest that the boundaries between particles in neutralized latex films remain intact and create a pathway for water transport. As such, in the drying process observed here, water loss is not impeded. Greater hydrophilicity at the particle boundaries is thereby expected to aid drying.

4. SUMMARY AND CONCLUSIONS

The effects of pH on the film drying, mechanical, and adhesive properties of a P(BuA-*co*-AA) latex film have been investigated. FTIR spectroscopy confirms that hydrogen bonds are formed by PAA carboxylic acid groups in the dried films cast at pH values lower than the pK_a of PAA. Ionized carboxylic acid groups are present in films cast at a pH above the pK_a and are neutralized by the counterion.

Macroscale tensile deformation and AFM nanomechanical measurements show that interparticle hydrogen bonding in the dried latex film does not affect the elastic modulus but increases the extension before failure. On the other hand, ionic dipolar interactions appear to impart a higher modulus and lower deformability in the dry films. The trends in the nanomechanical properties are consistent with the observed macroscale adhesive properties.

Probe–tack measurements illustrate that latex films from low-pH dispersions are more deformable and have a higher adhesion energy compared to films cast from high-pH dispersions. The adhesion energies of films cast at the various pH values can be explained by the bulk dynamic mechanical properties, using tan δ/E' as a criterion. Latex films cast at a pH of 4 have a lower E' but a higher tan δ, possibly because of energy dissipation in breaking the hydrogen bonds. On the other hand, latex films cast at a pH of 9 have a higher modulus, because of a stiffening attributed to the ionic dipolar interactions, but an intermediate tan δ. This work demonstrates a simple method to adjust the adhesive properties of a waterborne pressure-sensitive adhesive.

Although a low pH of the latex leads to a higher adhesion energy, it is relevant to note that the drying rate is slower, probably because water is trapped by hydrogen bonding with the AA groups. If fast drying is required for manufacturing, then a compromise might be found by raising the pH closer to the pK_a.

Acknowledgment. T.W. acknowledges an Overseas Research Student Scholarship from Universities U.K. and a University Research Scholarship from the University of Surrey. T.G.W. and E.C. acknowledge funding from the European Commission's Framework 6 Programme NAPOLEON project. We thank Prof. J. M. Asua and M. Manea at the Institute for Polymer Materials (POLYMAT), University of the Basque Country, Spain, for synthesis of the P(BuA-*co*-AA) latex and for useful discussions. We thank G. Cavalli (Surrey) for useful discussions and assistance with the FTIR spectroscopy.

REFERENCES AND NOTES

(1) Lakrout, H.; Creton, C.; Ahn, D.; Shull, K. R. *Macromolecules* **2001**, *34*, 7448–7458.
(2) do Amaral, M.; Roos, A.; Asua, J. M.; Creton, C. *J. Colloid Interface Sci.* **2005**, *281*, 325–338.
(3) Dos Santos, F. D.; Leibler, L. *J. Polym. Sci., Part B: Polym. Phys.* **2003**, *41*, 224–234.
(4) Wang, Y. C.; Kats, A.; Juhue, D.; Winnik, M. A.; Shivers, R. R.; Dinsdale, C. J. *Langmuir* **1992**, *8*, 1435–1442.
(5) Mallégol, J.; Dupont, O.; Keddie, J. L. *Langmuir* **2001**, *17*, 7022–7031.
(6) Tzitzinou, A.; Keddie, J. L.; Geurts, J. M.; Peters, A. C. I. A.; Satguru, R. *Macromolecules* **2000**, *33*, 2695–2708.
(7) Keddie, J. L. *Mater. Sci. Eng. R* **1997**, *21*, 101–170.
(8) Deplace, F.; Carelli, C.; Yamaguchi, T.; Foster, A.; Rabjohns, M. A.; Lovell, P. A.; Lei, C. H.; Keddie, J. L.; Ouzineb, K.; Creton, C. *Soft Matter* **2009**, in press. DOI: 10.1039/b815292f.
(9) Butler, L. N.; Fellows, C. M.; Gilbert, R. C. *Ind. Eng. Chem. Res.* **2003**, *42*, 456–464.
(10) Garrett, J.; Lovell, P. A.; Shea, A. J.; Viney, R. D. *Macromol. Symp.* **2000**, *151*, 487–496.
(11) Yang, Y. K.; Li, H.; Wang, F. *J. Adhes. Sci. Technol.* **2003**, *17*, 1741–1750.
(12) Joanicot, M.; Wong, K.; Richard, J.; Maquet, J.; Cabane, B. *Macromolecues* **1993**, *26*, 3168–3175.
(13) Mori, H.; Müller, A. H. E.; Klee, J. E. *J. Am. Chem. Soc.* **2003**, *125*, 3712–3713.
(14) Dong, J.; Ozaki, Y.; Nakashima, K. *Macromolecules* **1997**, *30*, 1111–1117.
(15) Kaczmarek, H.; Szalla, A.; Kamińska, A. *Polymer* **2001**, *42*, 6057–6069.

(16) Tsukida, N.; Muranaka, H.; Ide, M.; Maeda, Y.; Kitano, H. *J. Phys. Chem. B* **1997**, *101*, 6676–6679.
(17) Kim, B.; Peppas, N. A. *Polymer* **2003**, *44*, 3701–3707.
(18) Richard, J.; Maquet, J. *Polymer* **1992**, *33*, 4164–4173.
(19) Rharbi, Y.; Boue, F.; Joanicot, M.; Cabane, B. *Macromolecules* **1996**, *29*, 4346–4359.
(20) Kan, C. S.; Blackson, J. H. *Macromolecules* **1996**, *29*, 6853–6864.
(21) Feng, J. R.; Winnik, M. A. *Macromolecules* **1997**, *30*, 4324–4331.
(22) Reyes-Mercado, Y.; Vazquez, F.; Rodriguez-Gomez, F. J.; Duda, Y. *Colloid Polym. Sci.* **2008**, *286*, 603–609.
(23) Koh, A. Y. C.; Mange, S.; Bothe, M.; Leyrer, R. J.; Gilbert, R. G. *Polymer* **2006**, *47*, 1159–1165.
(24) Wang, T.; Lei, C. H.; Dalton, A. B.; Creton, C.; Lin, Y.; Fernando, K. A. S.; Sun, Y.-P.; Manea, M.; Asua, J. M.; Keddie, J. L. *Adv. Mater.* **2006**, *18*, 2730–2734.
(25) Burnham, N. A.; Colton, R. J. In *Scanning Probe Microscopy and Spectroscopy: Theory, Techniques, and Applications*, 2nd ed.; Bonnell, D., Ed.; Wiley-VCH: New York, 2001; Chapter 10, p 337.
(26) Akhremitchev, B. B.; Walker, G. C. *Langmuir* **1999**, *15*, 5630–5634.
(27) Shull, K. R. *Mater. Sci. Eng. R* **2002**, *36*, 1–45.
(28) Fretigny, C.; Basire, C.; Granier, V. *J. Appl. Phys.* **1997**, *82*, 43–48.
(29) Karian, H. G. *Handbook of Polypropylene and Polypropylene Composites*, 2nd ed.; CRC Press: Boca Raton, FL, 2003.
(30) Portigliatti, M.; Koutsos, V.; Hervet, H.; Léger, L. *Langmuir* **2000**, *16*, 6374–6376.
(31) Portigliatti, M.; Hervet, H.; Léger, L. *C. R. Acad. Sci. Paris Sér. IV* **2000**, 1187–1196.
(32) Paiva, A.; Sheller, N.; Foster, M. D.; Crosby, A. J.; Shull, K. R. *Macromolecules* **2000**, *33*, 1878–1881.
(33) Paiva, A.; Sheller, N.; Foster, M. D.; Crosby, A. J.; Shull, K. R. *Macromolecules* **2001**, *34*, 2269–2276.
(34) Kessel, N.; Illsley, D. R.; Keddie, J. L. *JCT Res.* **2008**, *5*, 285–297.
(35) Chiche, A.; Dollhofer, J.; Creton, C. *Eur. Phys. J. E* **2005**, *17*, 389–401.
(36) Zosel, A. *Int. J. Adhes. Adhes.* **1998**, *18*, 265–271.
(37) Lakrout, H.; Sergot, P.; Creton, C. *J. Adhes.* **1999**, *69*, 307–359.
(38) Shull, K. R.; Creton, C. *J. Polym. Sci., Part B: Polym. Phys.* **2004**, *42*, 4023–4043.
(39) Yamaguchi, T.; Doi, M. *Eur. Phys. J. E* **2006**, *21*, 331–339.
(40) Yamaguchi, T.; Koike, K.; Doi, M. *Europhys. Lett.* **2007**, *77*, 64002.
(41) Dimitrova, T. D.; Johannsmann, D.; Willenbacher, N.; Pfau, A. *Langmuir* **2003**, *19*, 5748–5755.
(42) Satas, D. *Handbook of Pressure Sensitive Adhesives*, 3rd ed.; Van Nostrand Reinhold: New York, 1989.
(43) Wang, T.; Lei, C. H.; Liu, D.; Manea, M.; Asua, J. M.; Creton, C.; Dalton, A. B.; Keddie, J. L. *Adv. Mater.* **2008**, *20*, 90–94.
(44) Nase, J.; Lindner, A.; Creton, C. *Phys. Rev. Lett.* **2008**, *101*, 074503.
(45) Basire, C.; Fretigny, C. *Eur. Phys. J. Appl. Phys.* **1999**, *6*, 323–329.

AM800179Y